This article was downloaded by:
On: *25 January 2011*
Access details: *Access Details: Free Access*
Publisher *Taylor & Francis*
Informa Ltd Registered in England and Wales Registered Number: 1072954 Registered office: Mortimer House, 37-41 Mortimer Street, London W1T 3JH, UK

Liquid Crystals
Publication details, including instructions for authors and subscription information:
http://www.informaworld.com/smpp/title~content=t713926090

Synthesis and characterization of new ferroelectric liquid crystals containing oligomethylene spacers

Yun Chen; Wei-Jen Wu

Online publication date: 06 August 2010

To cite this Article Chen, Yun and Wu, Wei-Jen(1998) 'Synthesis and characterization of new ferroelectric liquid crystals containing oligomethylene spacers', Liquid Crystals, 25: 3, 309 — 318
To link to this Article: DOI: 10.1080/026782998206100
URL: http://dx.doi.org/10.1080/026782998206100

PLEASE SCROLL DOWN FOR ARTICLE

Full terms and conditions of use: http://www.informaworld.com/terms-and-conditions-of-access.pdf

This article may be used for research, teaching and private study purposes. Any substantial or systematic reproduction, re-distribution, re-selling, loan or sub-licensing, systematic supply or distribution in any form to anyone is expressly forbidden.

The publisher does not give any warranty express or implied or make any representation that the contents will be complete or accurate or up to date. The accuracy of any instructions, formulae and drug doses should be independently verified with primary sources. The publisher shall not be liable for any loss, actions, claims, proceedings, demand or costs or damages whatsoever or howsoever caused arising directly or indirectly in connection with or arising out of the use of this material.

LIQUID CRYSTALS, 1998, VOL. 25, NO. 3, 309–318

Synthesis and characterization of new ferroelectric liquid crystals containing oligomethylene spacers

by YUN CHEN* and WEI-JEN WU

Department of Chemical Engineering, National Cheng Kung University, Tainan, Taiwan, ROC

(*Received 5 December 1997; in final form 21 February 1998; accepted 9 March 1998*)

Two series of ferroelectric liquid crystals containing a phenyl biphenyl carboxylate mesogenic group and oligomethylene spacers ($n = 3, 4, 6, 8$) were synthesized and characterized. The chiral moieties are the (*S*)-2-methylbutoxycarbonyl and (*S*)-1-methylheptoxycarbonyl groups. The mesomorphic behaviours of the compounds were characterized using differential scanning calorimetry and optical polarized microscopy. Spontaneous polarization ($\mathbf{P}_s$) of the liquid crystals was measured by an automated polarization tester over a wide temperature range. The mesomorphic properties are discussed as a function of spacer length and position of the chiral centre. It is found that the phase transition temperature decreases with increasing number of oligomethylene units. The phase behaviours of the LC with (*S*)-1-methylheptoxycarbonyl are more complex than those with (*S*)-2-methylbutoxycarbonyl, due to the flexible tail in the former. Moreover, the spontaneous polarization depends mainly on the position of the chiral centre, with $\mathbf{P}_s < 15\ \text{nC cm}^{-2}$ and $\mathbf{P}_s = 60 \sim 123\ \text{nC cm}^{-2}$ for the series with (*S*)-2-methylbutoxycarbonyl and (*S*)-1-methylheptoxycarbonyl groups, respectively.

Downloaded At: 19:46 25 January 2011

1. Introduction

Meyer *et al.* discovered ferroelectricity in the chiral smectic C (SmC*) phase in 1975 [1]; Clark and Lagerwall proposed electro-optical devices using ferroelectric liquid crystals (FLCs) in 1980 [2]. These discoveries have led to extensive studies on FLC materials because of their rapid switching time and their memory effect toward an applied electric field [3]. FLCs and ferroelectric liquid crystalline polymers (FLCPs) are studied extensively for display applications [4–8]. A FLC material used for a display should exhibit a smectic phase over a wide temperature range, including room temperature [9]. Moreover, the LC material must possess a large spontaneous polarization so that a FLC related device may be operated at a reduced driving voltage. These properties are influenced by the molecular structures of the liquid crystal compounds. It is thus of interest to synthesize FLC compounds which exhibit favourable spontaneous polarization values and smectic characteristics over a wide temperature range, especially room temperature. Besides low molar mass FLCs, several side chain liquid crystalline polymers (LCPs) exhibiting a chiral smectic C mesophase have been reported [10–13]; the ferroelectric properties of some of these LCPs have also been determined. FLCs containing oligo-oxyethylene spacers and various chiral moieties have been extensively studied by Hsiue *et al.* [14–17]; however, those with simple oligomethylene spacers have not so far been investigated.

In this work, we have synthesized and characterized two series of FLCs. The materials contain oligomethylene spacers, (*S*)-2-methylbutoxycarbonyl or (*S*)-1-methylheptoxycarbonyl chiral moieties, and three aromatic rings of ester core units. The influence of the spacer units and the different chiral tails on the formation of mesophases and spontaneous polarization is also discussed.

2. Synthesis

The compounds of series BM1*n* and BM2*n* were prepared as shown in the scheme. Detailed preparation procedures are described in § 5.

3. Results and discussion

The phase sequences and corresponding transition temperatures for these new series are listed in tables 1 and 2 and in figure 1.

3.1. *Optical microscopy*

3.1.1. *Series BM1n*

The four members of this series were composed of a (*S*)-2-methylbutoxycarbonyl chiral moiety and a methylene chain, in addition to a mesogen core of biphenyl and phenyl rings interconnected via an ester

*Author for correspondence.

0267–8292/98 $12·00 © 1998 Taylor & Francis Ltd.

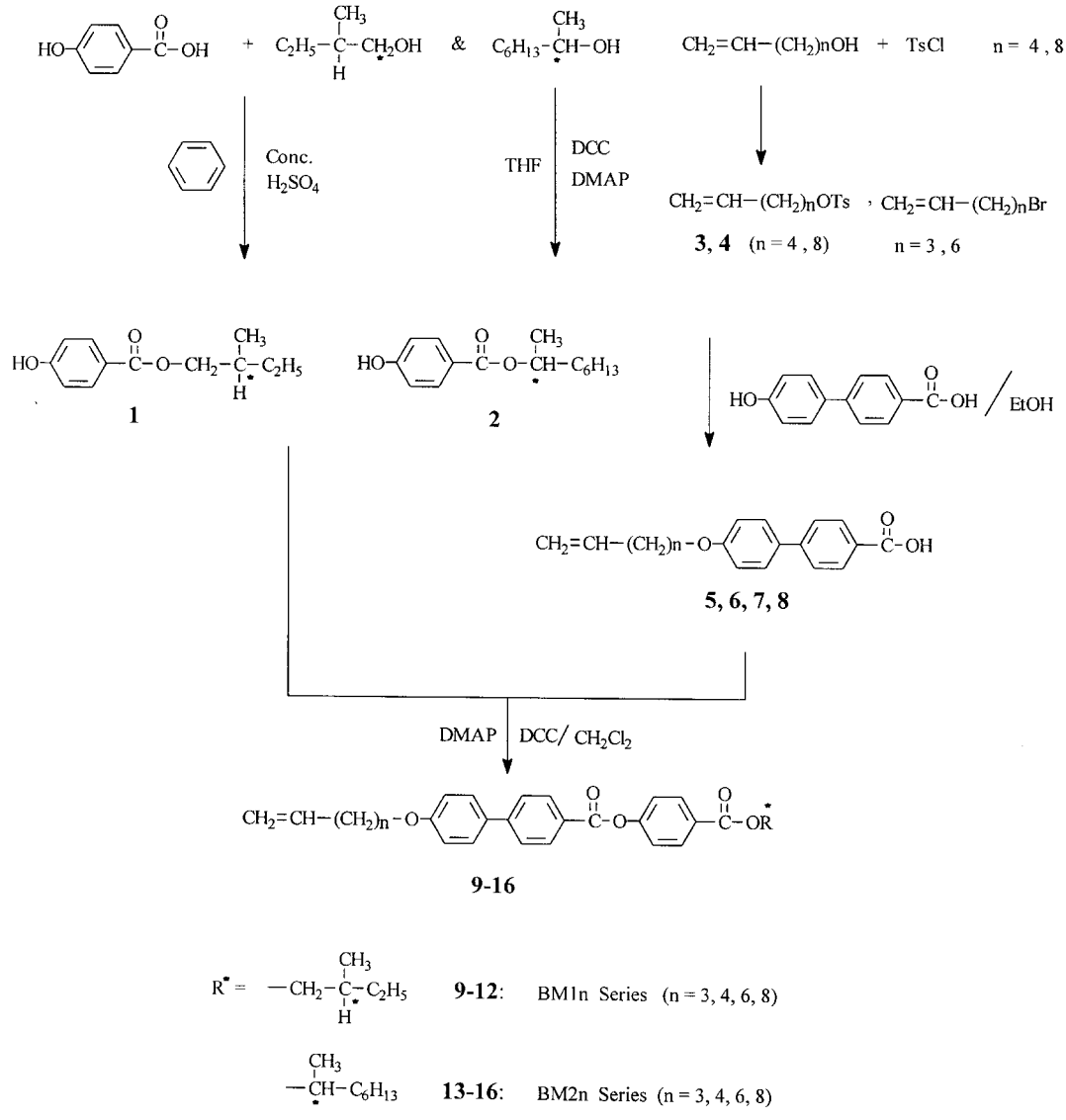

THF: tetrahydrofuran; DCC: N,N'-dicyclohexyl carbodiimide; DMAP: 4-(dimethyl amino) pyridine.

Scheme.

linkage. All the members exhibit a smectic A (SmA) phase. The first derivative BM13 which has three methylene units shows only an enantiotropic smectic A phase with focal-conic texture. However, BM14 and BM16 with 4 and 6 methylene units exhibit a monotropic smectic B (SmB) phase with enantiotropic SmA and chiral smectic C (SmC*) phases. On the other hand, for BM18 with a longer spacer chain ($n = 8$), the SmA, SmC*, and SmB phases are all enantiotropic.

Using BM18 as an example, upon cooling from the isotropic phase into the SmA phase, a focal-conic texture grows as shown in figure 2 (*a*). After further cooling to 134·2°C the SmC* phase appears, as evidenced by the formation of striated lines on the focal-conic fan texture or a broken fan texture [figure 2 (*b*)] due to the different pitch length at the various temperatures of the ferroelectric SmC* phase. The homeotropic region texture of the SmC* phase can also be observed [figure 2 (*c*)]. On subsequent cooling from the broken fan SmC* phase, a smectic B phase is indicated by the presence of a mosaic texture [figure 2 (*d*)].

Transition temperatures are plotted in figure 1 (*a*) as a function of n, the number of methylene units. As indicated in this figure, these methylene chains slightly depress the phase transition temperatures. The melting point of the crystalline phase also shows a tendency to

Downloaded At: 19:46 25 January 2011

Table 1. Phase transition temperatures and phase transition enthalpies for the series BM1*n*.

Identification	*n*[a]	Phase transition temperature/°C (enthalpy change/mJ mg^{-1})[b] Heating / Cooling
BM13	3	Cr 114·1(48·2) SmA 195·6(10·0) I I 189·2(9·1) SmA 82·8(41·9) Cr
BM14	4	Cr 85·3(41·2) SmC* 111·7(-)[c] SmA 188·0(9·4) I I 184·8(9·7) SmA 109·5(-)[c] SmC* 72·1(3·6) SmB 44·5(3·2) Cr
BM16	6	Cr 60·9(30·2) SmC* 141·9(-)[c] SmA 181·2(10·4) I I 176·7(9·5) SmA 139·8(-)[c] SmC* 55·8(1·9) SmB 28·9(13·2) Cr
BM18	8	Cr 42·2(14·2) SmB 53·9(1·2) SmC* 138·7(0·2) SmA 175·7(9·0) I I 170·8(9·5) SmA 134·2(0·3) SmC* 47·3(2·4) SmB 14·5(13·7) Cr

[a] *n* is the number of methylene units as shown in the scheme.
[b] Cr = crystalline phase, SmA = smectic A phase, SmC* = chiral smectic C phase, SmB = smectic B phase, I = isotropic phase.
[c] Enthalpies were too small to be evaluated.

Table 2. Phase transition temperature and phase transition enthalpies for the series BM2*n*.

Identification	*n*[a]	Phase transition temperature/°C (enthalpy change/mJ mg^{-1})[b] Heating / Cooling
BM23	3	Cr 118·1(51·8) SmA 166·5(11·4) I I 161·4(11·5) SmA 81·0(44·7) Cr
BM24	4	Cr 79·1(18·9) SmC* 92·1(38·3) SmA 155·5(11·5) I I 151·4(13·1) SmA 80·2(2·8) SmC* 58·6(4·4) CrE 34·5(24·6) Cr
BM26	6	Cr 83·8(70·1) CrE 86·9(-)[c] SmC* 118·3(0·2) SmX 120·1(-)[c] SmA 141·6(9·2) I I 137·0(8·7) SmA 115·2(-)[c] SmX 113·3(0·4) SmC* 78·5(-)[c] CrE 47·5(54·6) Cr
BM28	8	Cr 54·0(49·2) CrE 62·7(-)[c] SmC* 121·1(0·8) SmX 122·3(-)[c] SmA 134·5(18·1) I I 132·2(8·4) SmA 120·9(-)[c] SmX 119·3(1·0) SmC* 50·7(-)[c] CrE 42·0(1·7) SmY −7·4(4·1) Cr

[a] *n* is the number of methylene units as shown in the scheme.
[b] Cr = crystalline phase, SmA = smectic A phase, SmC* = chiral smectic C phase, CrE = smectic E phase, SmX = unidentified smectic phase, SmY = unidentified smectic phase, I = isotropic phase.
[c] Enthalplies were too small to be evaluated.

Downloaded At: 19:46 25 January 2011

fall with the number of methylene units; this depression is attributed to the increasing flexibility of the C–C bonds. For $n = 3$ only a SmA liquid crystalline phase can be observed, while for $n \geqslant 4$ two more phases, SmC* and SmB, appear. The SmC* phase ranges increase significantly as the number of methylene units increases, while those of SmB show only a slight increase; however, the SmA phase displays an opposite trend.

3.1.2. *Series BM2n*

The chemical structure of this series differs from that of series BM1*n* only in its chiral moiety, i.e. it uses the (*S*)-1-methylheptoxycarbonyl chiral group instead of the (*S*)-2-methylbutoxycarbonyl group. Therefore, the chiral centre is much closer to the mesogenic core for series BM2*n*; table 2 depicts its phase sequences and transition temperatures. All the four members exhibit an enantiotropic SmA phase. Enantiotropic SmC* and monotropic CrE phases can also be observed for BM24 with four methylene units. However, for BM26 and BM28 both the SmC and CrE phases are enantiotropic. In addition, BM28 contains a more ordered monotropic smectic (SmX) phase, which needs further identification.

As in series BM1*n*, the smectic A phase occurs in all four derivatives. The enantiotropic SmC* phase is present in three ($n = 4, 6, 8$) of the homologues. For example, derivative BM26 exhibits all enantiotropic smectic A, chiral smectic C and CrE phases, as well as an unidentified smectic phase SmX, as shown in figure 3. Derivative BM28 shows similar mesophases to those of BM26 except for the presence of an additional unidentified smectic SmY phase.

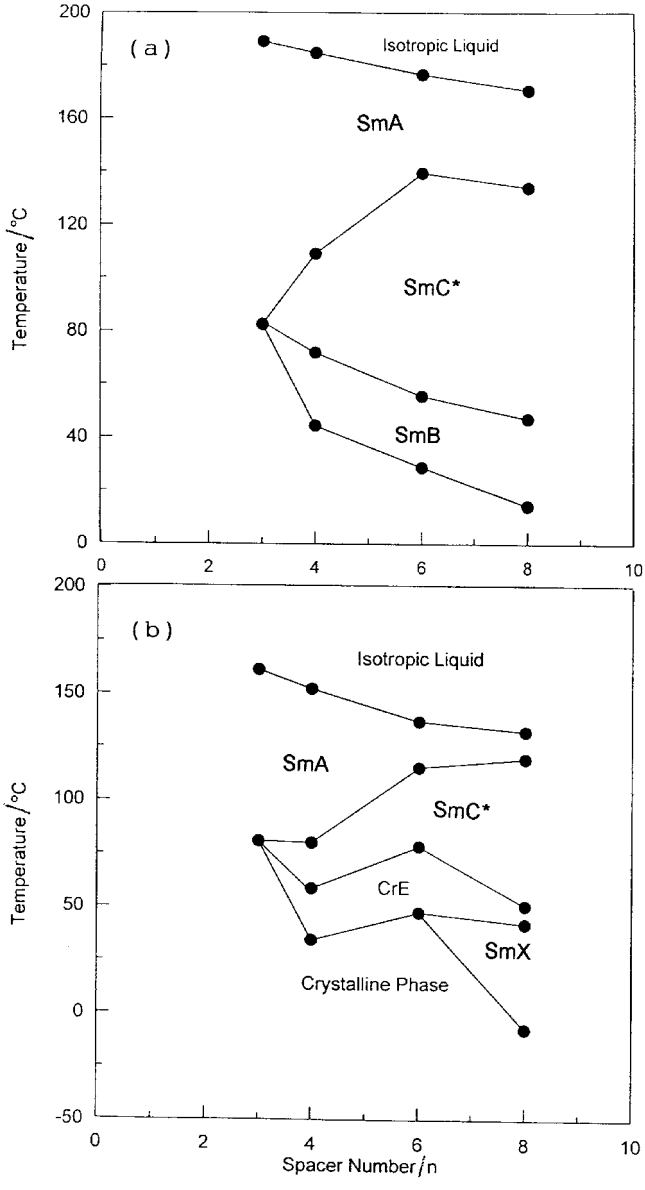

Figure 1. Plots of transition temperature versus n, the number of oxymethylene units: (*a*) BM1*n*; (*b*) BM2*n*.

The transition temperatures of BM2*n* are plotted in figure 1 (*b*) as a function of n, the number of methylene units. As indicated in this figure, these methylene chains slightly depress the phase transition temperatures, this depression being ascribed to the increasing flexibility of the C–C bonds. As with the BM1*n* series, for $n=3$ only a SmA liquid crystalline phase can be observed, while for $n=4$ and 6 two more phases, SmC* and CrE, appear. Furthermore, for $n=8$ a new ordered phase appears below 50°C, but has not yet been identified. The SmC* phase ranges increase significantly as the number of methylene units increases, while those of the CrE phase show at first an increase and then a decrease at $n=8$. However, the SmA phase range displays an opposite trend, i.e. it narrows greatly as n is increased from 3 to 8.

Results shown in figures 1 (*a*) and 1 (*b*) indicate that compounds of the series BM2*n* exhibit different liquid crystalline behaviour from those of the series BM1*n*, i.e. the SmB phase in BM1*n* is replaced by CrE and SmX phases. Moreover, the temperature ranges of the SmA and SmC* phases of BM2*n* are narrower than those of series BM1*n*. These trends seem due to the more flexible chiral moiety in BM2*n*.

3.2. *Calorimetric studies*

Transition enthalpies were determined by differential scanning calorimetry (DSC) using a Shimadzu DSC-50. The transition temperatures and corresponding enthalpy values of series BM1*n* and BM2*n* are listed in tables 1 and 2, respectively. The thermograms were recorded on cooling at a rate of 10°C min^{-1}. For BM14 and BM16, individual transition enthalpies for the SmC*/SmX transitions are too small to be determined (figure 4). Other transition enthalpies can be determined unambiguously. For BM26 and BM28, the transition enthalpies for the CrE/SmC* and SmX/SmA transitions can also not be determined due to their low values (figure 5). Some compounds of the two series undergo a larger degree of supercooling, with a maximum of about 60°C for BM28.

3.3. *Spontaneous polarization*

Spontaneous polarizations ($\mathbf{P}_S$) of the BM1*n* and BM2*n* ($n=4, 6, 8$) were determined in a LC cell made of ITO coated glass whose surface had been treated with a parallel alignment of polyimide. The helical alignment of SmC* is unwound by annealing around the isotropic temperature (T_I) and becomes a parallel alignment along the treated direction, as shown in figure 6 for BM16. Spontaneous polarization values were taken after slow cooling to the SmC* temperature range.

3.3.1. *Series BM1n*

This series of compounds are ferroelectric liquid crystals with (*S*)-2-methylbutoxycarbonyl as the asymmetric centre, in which the chiral centre is located at the β-carbon. The $\mathbf{P}_S$ values depend on temperature and exhibit a maximum, as shown in figure 7 (*a*). The maximum $\mathbf{P}_S$ values are 11·1 (at 100°C), 13·3 (95°C), and 3·5 nC cm^{-2} (85°C) for BM14, BM16, and BM18, respectively. The first increase in $\mathbf{P}_S$ value with decreasing temperature below T_I can be attributed to decreased thermal motion at the lower temperature. After maximum $\mathbf{P}_S$ is reached, continued lowering of the temperature results in a decreasing $\mathbf{P}_S$, which may be due to

Downloaded At: 19:46 25 January 2011

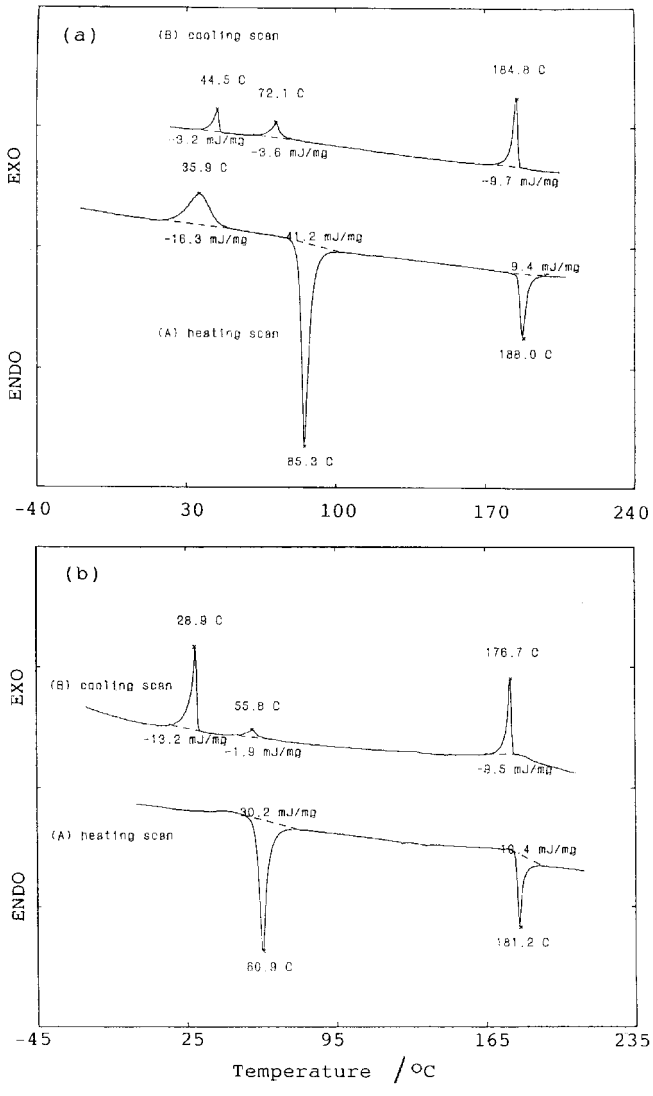

Figure 4. DSC thermograms of (*a*) BM14 and (*b*) BM16.

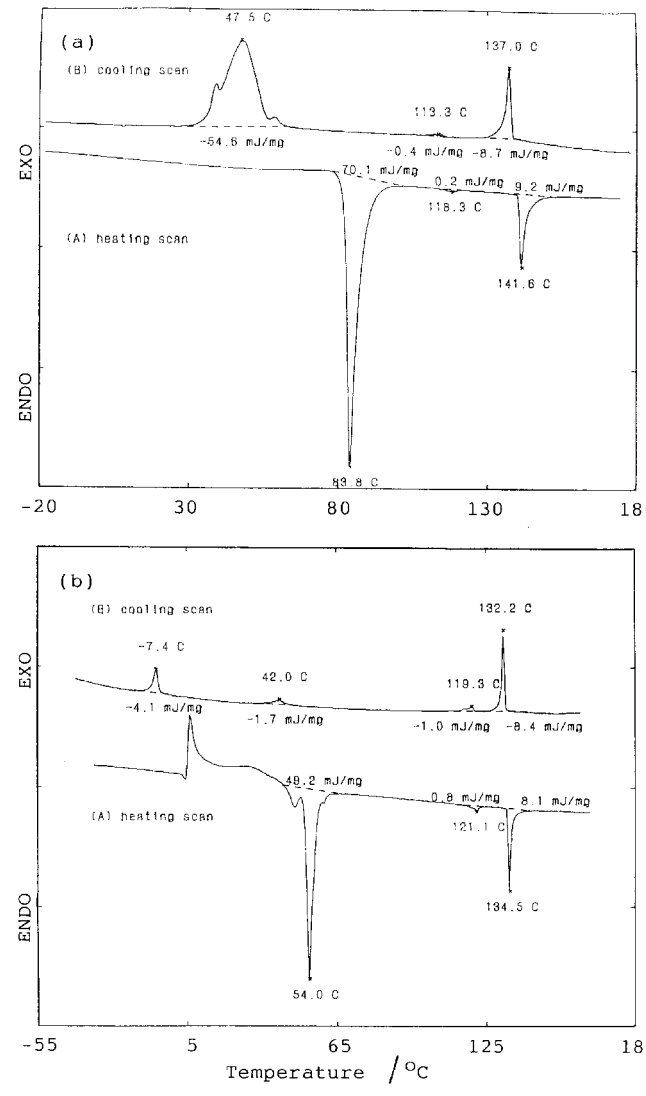

Figure 5. DSC thermograms of (*a*) BM26 and (*b*) BM28.

crystallization. In general, the $\mathbf{P}_S$ values of this series are small and lower than 13·3 nC cm^{-2}.

3.3.2. *Series BM2n*

The chiral centre of this series is (*S*)-1-methylheptoxycarbonyl and located at the α-position of the heptyl chain. The $\mathbf{P}_S$ value versus temperature plot is shown in figure 7 (*b*). The ferroelectric liquid crystals BM24, BM26, and BM28 exhibit maximum $\mathbf{P}_S$ values of 62·2 (at 65°C), and 123 nC cm^{-2} (72°C), respectively. As with the BM1*n* series, the $\mathbf{P}_S$ values first increase with decreasing temperature from T_I and then decrease after a maximum value.

In general, it is found that the $\mathbf{P}_S$ value depends on the location of the chiral centre: the closer the chiral centre to the mesogenic core, the greater the $\mathbf{P}_S$ value. Accordingly, series BM2*n* compounds exhibit much greater $\mathbf{P}_S$ values (62·2–123 nC cm^{-2}) than compounds of series BM1*n* (3·5–13·3 nC cm^{-2}). This is attributable to the greater dipole moment of the SmC* phase when the chiral centre is closer to the mesogenic core and can stabilize the C_2 symmetric LC phase.

4. Conclusions

New ferroelectric liquid crystals containing a phenyl biphenyl carboxylate mesogenic core, oligomethylene spacer and two different chiral moieties, (*S*)-2-methylbutoxycarbonyl and (*S*)-1-methylheptoxycarbonyl have been synthesized. All the compounds display liquid crystalline phases. The spacer chain of methylene units favours a lowering of transition temperatures and an increasing temperature range of the SmC* phase. Our results indicate that the BM1*n* series show only enantiotropic SmA phases. BM14 and BM16 exhibit additional

Downloaded At: 19:46 25 January 2011

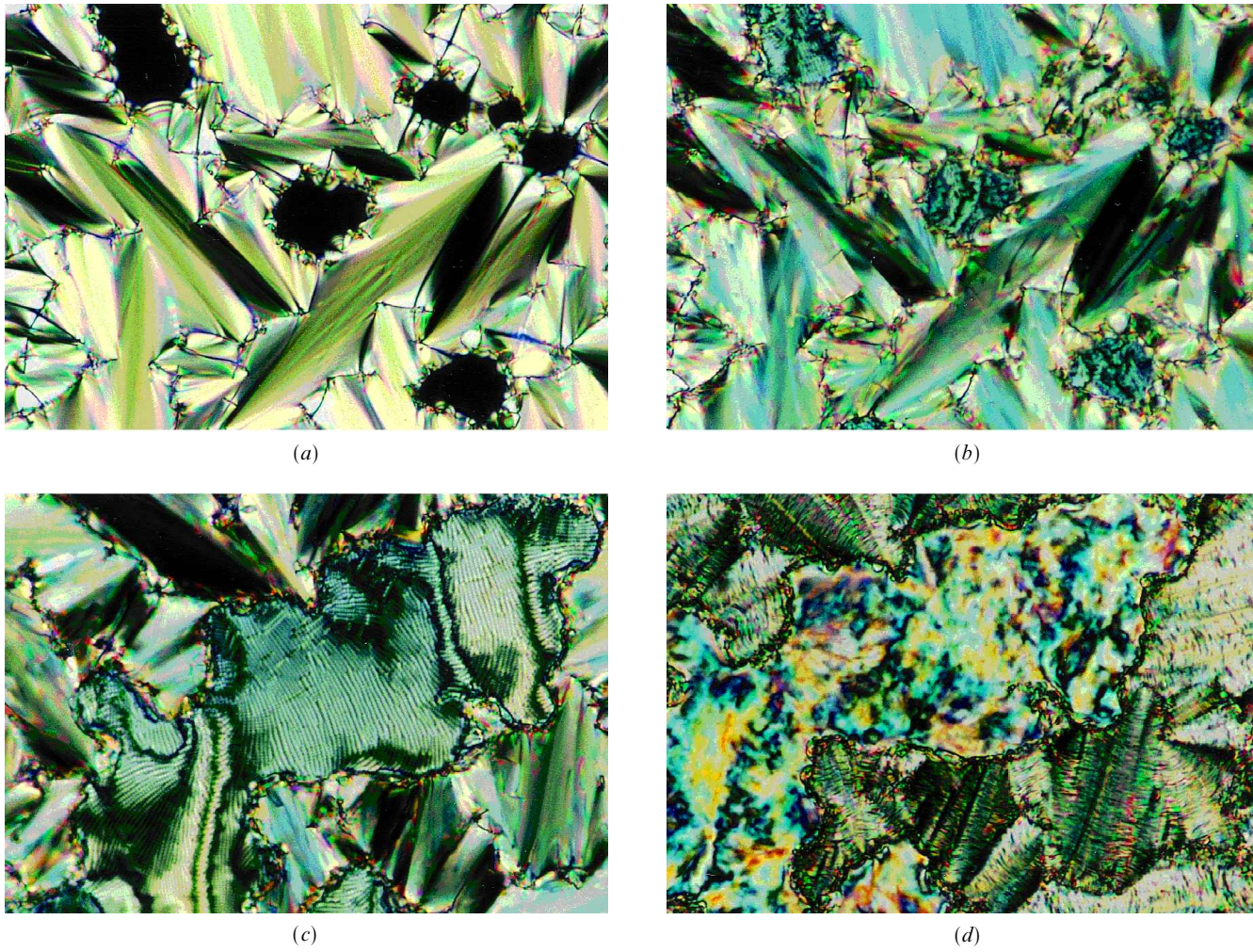

(*a*) (*b*)

(*c*) (*d*)

Figure 2. Optical polarizing microscopy of MB18 (×100): (*a*) the SmA phase at 143°C; (*b*) the SmC* phase at 133°C; (*c*) the homotropic region of SmC* phase at 133°C; (*d*) the SmB phase at 42°C.

Downloaded At: 19:46 25 January 2011

enantiotropic SmC* and monotropic SmB phases. However, in BM18 all the LC phases, SmA, SmC* and SmB are enantiotropic. The temperature ranges of the SmC* and SmB phases increase with spacer length. Spontaneous polarization values are smaller than 13·3 nC cm^{-2}. For series BM2*n*, all members also show the enantiotropic SmA phase; the SmC* and CrE phases appear when the spacer length is increased. The $\mathbf{P}_S$ values of the BM2*n* series in the FLC phase show maxima between 62·2 and 123 nC cm^{-2}, which are much greater than those of the series BM1*n* (3·5–13·3 nC cm^{-2}). The $\mathbf{P}_S$ results imply that the (*S*)-1-methylheptoxycarbonyl chiral tail enhances the spontaneous polarization.

5. Experimental

5.1. *Materials*

4-(4′-Hydroxyphenyl)benzoic acid, (*S*)-2-methyl-1-butanol, (*S*)-1-methyl-1-heptanol, 8-bromo-1-octene and 5-bromo-1-pentene (from TCI), 5-hexen-1-ol, 9-decen-1-ol, 4-hydroxybenzoic acid (from Wako), and other reagents (from Merck) were used without further purification. Solvents were dried by refluxing with CaH_2 under a nitrogen blanket, then distilled and stored with 4 Å molecular sieves before use.

5.2. *Measurements*

^{1}H NMR spectra were obtained with a Bruker AM-200 MHz or 400 MHz spectrometer. All spectra were recorded on $CDCl_3$ solutions with tetramethylsilane (TMS) as internal standard unless otherwise noted. A Shimadzu DSC-50 differential scanning calorimeter equipped with a computer system was used to determine thermal transitions, read at the maximum of their endothermic or exothermic peaks. In all cases, heating and cooling rates were 10°C min^{-1}, unless otherwise specified. After the first heating scan, the sample was

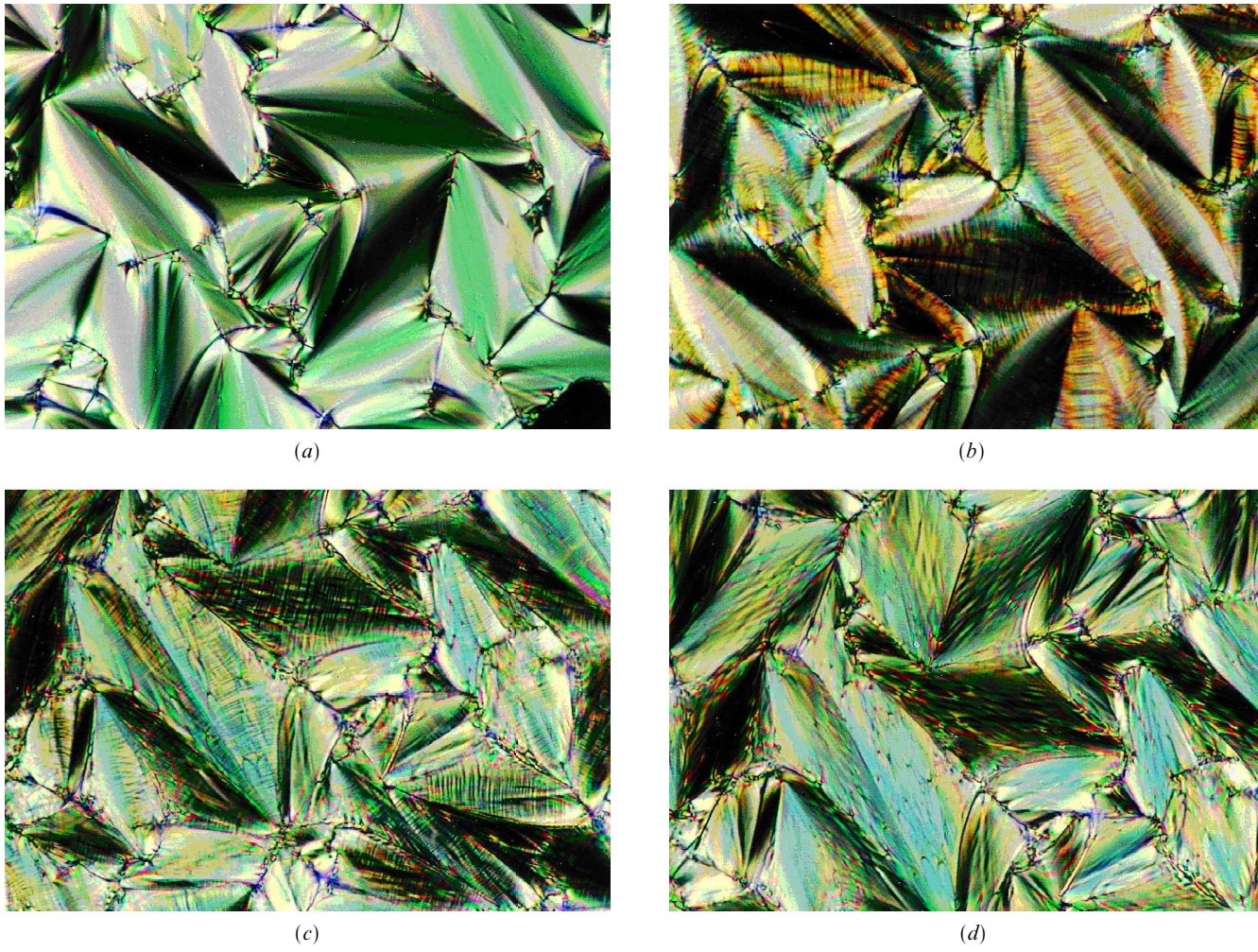

(*a*) (*b*)

(*c*) (*d*)

Figure 3. Optical polarizing microscopy of MB26 (×100): (*a*) the SmA phase at 133°C; (*b*) the unidentified phase at 115°C; (*c*) the SmC* phase at 101°C; (*d*) the CrE phase at 70°C.

Downloaded At: 19:46 25 January 2011

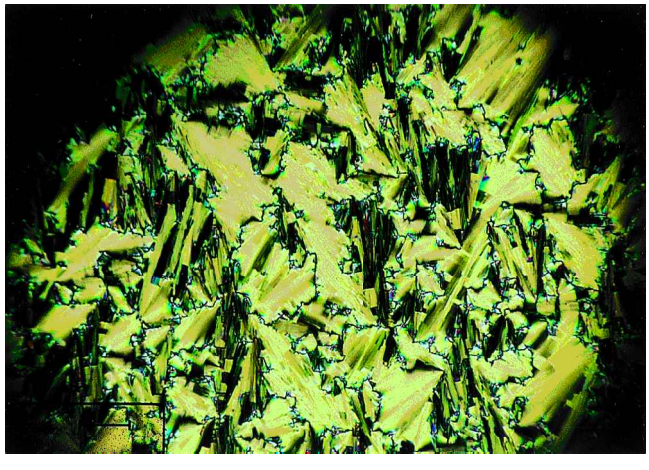

Figure 6. The homogeneous alignment texture of the SmA phase of BM16 at 67°C (×200).

annealed at 10°C above the isotropization temperature for 5–10 min. Under these conditions, the second heating and cooling scans all recorded reproducible data. The transitions reported were taken during the second or third heating and cooling scans unless otherwise specified. A Nikon Microphot-FX optical polarizing microscope equipped with a Mettler FP-82 hot stage and a Mettler FP-80 central processor was used to observe the thermal transitions and isotropic textures. Optical rotations were measured at ambient temperature on a Jasco DIP-370 digital polarimeter with chloroform as the solvent for all compounds. Spontaneous polarization values of the FLCs were determined by an automated polarization tester, model APT III, from Displaytech. The liquid crystal cells (4 μm thick), also from Displaytech, were made of ITO glass coated with polyimide, which was parallel rubbed; a 15 V μm^{-1} potential was applied and

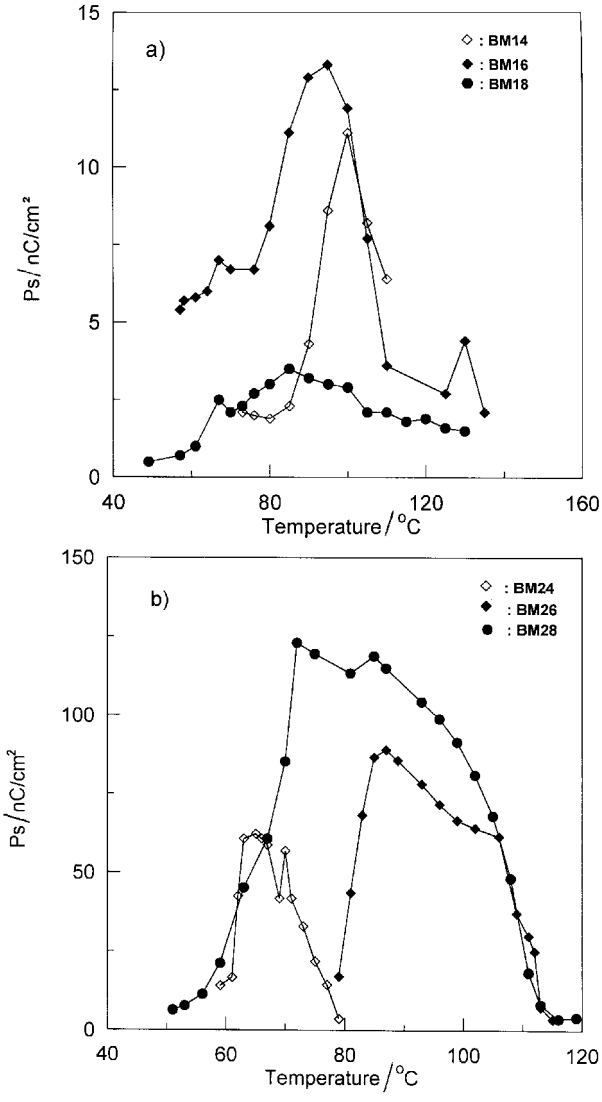

Figure 7. Spontaneous polarization ($\mathbf{P}_S$) versus temperature for (*a*) BM1*n* and (*b*) BM2*n*.

the measuring frequency was 100 Hz [18]. The samples were first heated to isotropic temperature and then cooled slowly to the chiral smectic C phase, during which process spontaneous polarizations were recorded successively.

5.3. *Synthesis*

5.3.1. *(S)-2-Methyl-1-butyl 4-hydroxybenzoate (**1**)*

In a 100 ml, round-bottom flask equipped with a magnetic stirrer were placed (*S*)-2-methyl-1-butanol (13·208 g, 0·15 mol), 4-hydroxybenzoic acid (13·851 g, 0·1 mol) and 50 ml dried benzene. After adding several drops of concentrated sulphuric acid, the mixture was allowed to boil under reflux at 90°C until complete esterification, as traced by TLC had taken place. The solution was washed successively with 5% sodium carbonate aqueous solution and deionized water. The solids, obtained by evaporating the solvent, were purified by open column chromatography. Yield 80·4%, ^{1}H NMR ($CDCl_3$, TMS) δ 0·85–1·05 (m, 6H, –C**H**$_3$), 1·20–1·58 (m, 2H, –C**H**$_2$), 1·78–1·91 (m, 1H, –C**H**–), 4·14 (m, 2H, –COOHC**H**$_2$), 6·90–7·90 ppm (2d, 4H, aromatic protons).

5.3.2. *(S)-1-Methyl-1-heptyl 4-hydroxybenzoate (**2**)*

Compound **2** was obtained from the esterification of (*S*)-1-methyl-1-heptanol and 4-hydroxybenzoic acid. In a two-neck glass reactor was placed 4-hydroxybenzoic acid (5·016 g, 0·036 mol), (*S*)-1-methyl-1-heptanol (5·224 g, 0·039 mol), and 100 ml dried tetrahydrofuran (THF). The mixture was purged with nitrogen and allowed to react at room temperature after adding *N*,*N*-dicyclohexylcarbodiimide (DCC; 8·426 g, 0·04 mol) and several drops of dimethylaminopyridine (DMAP). TLC confirmed the completion of the esterification. The products were purified by column chromatography using ethyl acetate/*n*-hexane (v/v = 8/1) as eluent. Yield 79·5%, ^{1}H NMR ($CDCl_3$, TMS) δ 0·9 [t, 3H, –$(CH_2)_4$–C**H**$_3$], 1·34 (d, 3H, –OCHC**H**$_3$–), 1·26–2·28 [m, 10H, –$(CH_2)_5$–CH_3], 4·44 (m, 1H, –O–C**H**CH_3–CH_2–), 5·35 (s, 1H, **H**O–), 6·9 and 8·05 ppm (2d, 4H, aromatic protons).

5.3.3. *5-Hexenyl tosylate (**3**), 9-decenyl tosylate (**3**)*

For the preparation of compound **3**, into a two-necked glass reactor at 0°C containing 5-hexen-1-ol (7·004 g, 0·07 mol) in 30 ml dried pyridine, was added dropwise a solution formed by dissolving *p*-toluene sulphonyl chloride (14·656 g, 0·077 mol) in 30 ml dried pyridine. The mixture was allowed to react for about 8 h, then mixed with 70 ml chilled water. After extracting with ethyl ether, the organic phase was washed successively with 6N HCl, water, saturated aqueous sodium carbonate, and water. The colourless liquid product was obtained in evaporating the solvent.

Compound **4** was prepared by an analogous process.

3: Yield 82·4%, ^{1}H NMR ($CDCl_3$, TMS) δ 1·20–2·00 [m, 4H, CH_2=$CHCH_2$(C**H**$_2$)$_2$$CH_2$O], 2·35–2·43 (s, 3H, –C**H**$_3$), 3·45–3·55 [m, 2H, CH_2=$CHCH_2$$(CH_2)_2$C**H**$_2$O], 4·80–5·00 (m, 2H, C**H**$_2$=$CHCH_2$$(CH_2)_2$$CH_2$O) 5·80–6·05 [m, 1H, CH_2=C**H**$CH_2$$(CH_2)_2$$CH_2$O], 7·20–7·70 ppm (2d, 4H, aromatic protons).

4: Yield 92·3%, ^{1}H NMR ($CDCl_3$, TMS) δ 1·20–2·00 [m, 12H, CH_2=$CHCH_2$(C**H**$_2$)$_6$$CH_2$O], 2·35–2·43 (s, 3H, –C**H**$_3$), 3·45–3·55 [m, 2H, CH_2=$CHCH_2$$(CH_2)_6$C**H**$_2$O], 4·80–5·00 [m, 2H, C**H**$_2$=$CHCH_2$$(CH_2)_6$$CH_2$O], 5·80–6·05 [m, 1H, CH_2=C**H**$CH_2$$(CH_2)_6$$CH_2$O], 7·20–7·70 ppm (2d, 4H, aromatic protons).

Downloaded At: 19:46 25 January 2011

5.3.4. *4-(4-Penten-1-yloxy)biphenyl-4′-carboxylic acid (**5**), 4-(7-octen-1-yloxy)biphenyl-4′-carboxylic acid (**7**)*

For the preparation of compound **7**, 70 ml ethanol were mixed with 4-(4′-hydroxyphenyl)benzoic acid (2·586 g, 0·012 mol), potassium hydroxide (2·029 g, 0·037 mol), and 0·205 g potassium iodide (0·2058, 0·0012 mol). The mixture was allowed to react for 6 h at 70°C, then 8-bromo-1-octene (5·356 g, 0·026 mol) was added dropwise and the mixture continued to react for another 15 h. After cooling to ambient temperature, 350 ml water was added and the mixture neutralized with 6N HCl to slight acidic conditions: it was then extracted with THF, and light yellow solids were obtained after evaporating the solvent. Recrystallization in THF and *n*-hexane isolated product **7**.

Compound **5** was prepared by an analogous process. **5**: Yield 53·9%, ^{1}H NMR ($CDCl_3$, TMS) δ 1·20–2·10 [m, 4H, $-(CH_2)_2-$], 3·90–4·00 [t, 2H, $-O-CH_2-(CH_2)-$], 4·90–5·10 (m, 2H, $CH_2=CH-$), 5·70–5·90 (m, 1H, $CH_2=CH-$), 6·90–8·20 ppm (m, 8H, aromatic protons).

Table 3. The yields, chemical shift δ/ppm values, and $[\alpha]_D^{25}$ of series BM1*n* and BM2*n*.

Compound	Identification	Yield/%	$[\alpha]_D^{25}$[a]	^{1}H NMR spectra[b]
9	BM13	72·3	+1·9	0·93–1·04 (m, 6H, $-(CH_3)$ and $-CH_2CH_3$), 1·25–1·36 (m, 2H, $-CH_2CH_3$), 1·83–2·00 (m, 3H, CH and $-OCH_2CH_2-$), 2·23–2·33 (m, 2H, $CH_2=CH-CH_2-$), 4·00–4·10 (t, 2H, $PhOCH_2-$), 4·13–4·27 (m, 2H, $-COOCH_2-$), 5·00–5·14 (m, 2H, $CH_2=$), 5·70–5·90 (m, 1H, $=CH-$), 6·98–8·26 (6d, 12H, aromatic protons).
10	BM14	75·6	+5·0	0·93–1·04 (m, 6H, $-(CH_3)$ and $-CH_2CH_3$), 1·26–1·37 (m, 2H, $-CH_2CH_3$), 1·55–1·63 (m, 2H, $-(CH_2)-$), 1·78–1·88 (1m, 3H, CH and $-OCH_2CH_2-$), 2·13–2·25 (m, 2H, $CH_2=CHCH_2-$), 4·00–4·10 (t, 2H, $PhOCH_2-$), 4·13–4·25 (m, 2H, $-COOCH_2-$), 4·97–5·10 (m, 2H, $CH_2=$), 5·70–5·98 (m, 1H, $=CH-$), 6·99–8·26 (6d, 12H, aromatic protons).
11	BM16	76·9	+4·6	0·97–1·05 (m, 6H, $-CH(CH_3)$ and $-CH_2CH_3$), 1·21–1·51 (m, 2H, $-CH_2CH_3$), 1·30–60 (m, 6H, $-(CH_2)_3-$), 1·79–1·97 (m, 3H, CH and $-OCH_2CH_2-$), 2·03–2·15 (m, 2H, $CH_2=CHCH_2-$), 4·02–4·10 (t, 2H, $PhOCH_2-$), 4·13–4·25 (m, 2H, $-COOCH_2-$), 4·95–5·10 (m, 2H, $CH_2=$), 5·75–5·93 (m, 1H, $=CH-$), 6·99–8·22 (6d, 12H, aromatic protons).
12	BM18	81·8	+3·8	0·93–1·04 (m, 6H, $-CH(CH_2)$ and $-CH_2CH_3$), 1·23–1·57 (m, 12H, $-CH_2CH_3$ and $-(CH_2)_5-$), 1·75–1·89 (m, 3H, CH and $-OCH_2CH_2-$), 2·03–2·13 (m, 2H, $CH_2=CHCH_2-$), 3·99–4·13 (t, 2H, $PhOCH_2-$), 4·14–4·25 (m, 2H, $-COOCH_2-$), 4·91–5·04 (m, 2H, $CH_2=$), 5·75–5·95 (m, 1H, $=CH-$), 6·99–8·26 (6d, 12H, aromatic protons).
13	BM23	62·3	+26·6	0·84–0·88 (t, 3H, $-(CH_2)_5-CH_3$), 1·25–1·67 (m, 10H, $-(CH_2)_5-CH_3$), 1·89–1·95 (m, 3H, $-OCH(CH_3)$), 2·22–2·29 (q, 2H, $CH_2=CH-CH_2$), 4·00–4·07 (t, 2H, $PhOCH_2-$), 5·00–5·18 (m, 3H, $CH_2=CH$ and $-OCH(CH_3)-$), 5·85–6·00 (m, 1H, $CH_2=CH$), 6·99–8·26 (6d, 12H, aromatic protons).
14	BM24	65·7	+24·6	0·85–0·88 (t, 3H, $-(CH_2)_5-CH_3$), 1·25–1·67 (m, 12H, $-(CH_2)_5CH_3$ and $CH_2=CH-CH_2-CH_2$), 1·78–2·10 (m, 5H, $-OCH(CH_3)$ and $PhOCH_2-CH_2-$), 2·13–2·21 (q, 2H, $CH_2=CH-CH_2$), 4·00–4·06 (t, 2H, $PhOCH_2-$), 4·97–5·18 (m, 3H, $CH_2=CH-$ and $-OCH(CH_3)-$), 5·83–5·93 (m, 1H, $CH_2=CH$), 6·98–8·26 (6d, 12H, aromatic protons).
15	BM26	73·5	+25·0	0·85–0·91 (t, 3H, $-(CH_2)_5-CH_3$), 1·25–1·56 (m, 16H, $-(CH_2)_5-CH_3$ and $CH_2=CH-CH_2-(CH_2)_3-$), 1·56–1·81 (m, 5H, $-OCH(CH_3)$ and $PhOCH_2-CH_2-$), 2·05–2·07 (q, 2H, $CH_2=CH-CH_2-$), 3·98–4·02 (t, 2H, $PhOCH_2-$), 4·90–5·10 (m, 2H, $CH_2=CH-$), 5·11–5·22 (m, 1H, $-OCH(CH_3)-$), 5·78–5·90 (m, 1H, $CH_2=CH$), 6·97–8·23 (6d, 12H, aromatic protons).
16	BM28	61·7	+20·2	0·85–0·88 (t, 3H, $-(CH_2)_5-CH_3$), 1·29–1·58 (m, 20H, $-(CH_2)_5-CH_3$ and $CH_2=CH-CH_2-(CH_2)_5-$), 1·63–1·85 (m, 5H, $-OCH(CH_3)$ and $PhOCH_2-CH_2-$), 3·99–4·05 (t, 2H, $PhOCH_2$), 4·91–5·04 (m, 2H, $CH_2=CH-$), 5·12–5·18 (m, 1H, $CH_2=CH$), 6·97–8·26 (6d, 12H, aromatic protons).

[a] These values were measured in $CHCl_3$ at 25°C.
[b] These values were measured in $CDCl_3$, using 200 or 400 MHz nuclear magnetic resonance spectroscopy.

Downloaded At: 19:46 25 January 2011

7: Yield 60·6%, ^{1}H NMR ($CDCl_3$, TMS) δ 1·20–2·10 [m, 10H, $-(CH_2)_5-$], 3·90–4·00 [t, 2H, $-OCH_2-(CH_2)_5-$], 4·90–5·10 (m, 2H, $CH_2=CH-$), 5·70–5·90 (m, 1H, $CH_2=CH-$), 6·90–8·20 ppm (m, 8H, aromatic protons).

5.3.5. *4-(5-Hexen-1-yloxy)biphenyl-4′-carboxylic acid (**6**), 4-(9-decen-1-yloxy)biphenyl-4′-carboxylic acid (**8**)*

Using compound **6** as an example, to a two-necked glass reactor were added 4-(4′-hydroxyphenyl)benzoic acid (5·356 g, 0·025 mol), potassium hydroxide (4·39 g, 0·08 mol), potassium iodide (0·225 g, 0·0014 mol), and 100 ml ethyl alcohol. The mixture was allowed to react at 70°C for 3 h. Compound **3** (6·999 g, 0·0275 mol) was then added dropwise to the reactor and the mixture continued to react for another 20 h. The white precipitate obtained appearing after cooling and neutralizing with 6N HCl to slight acidic condition, was collected by filtration; the solid was purified by recrystallization from ethyl alcohol and water.

6: Yield 80·3%, ^{1}H NMR ($CDCl_3$, TMS δ 1·20–2·10 [m, 6H, $-(CH_2)_3-$], 3·90–4·00 [t, 2H, $-O-CH_2-(CH_2)_2-$], 4·90–5·10 (m, 2H, $-CH_2=CH-$), 5·70–5·90 (m, 1H, $-CH_2=CH-$), 6·90–8·20 ppm (m, 8H, aromatic protons).

8: Yield 86·4%, ^{1}H NMR ($CDCl_3$, TMS) δ 1·20–2·10 [m, 14H, $-(CH_2)_7-$], 3·90–4·00 [t, 2H, $-O-CH_2-(CH_2)_7-$], 4·90–5·10 (m, 2H, $-CH_2=CH-$), 5·70–5·90 (m, 1H, $-CH_2=CH-$), 6·90–8·20 ppm (m, 8H, aromatic protons).

5.3.6. *4-(S)-2-Methyl-1-butyl [4-(4-penten-1-yloxy)-biphenyl-4′-carbonyloxy]benzoate (**9**), 4-(S)-2-methyl-1-butyl [-(5-hexen-1-yloxy)-biphenyl-4′-carbonyloxy]benzoate (**10**), 4-(S)-2-methyl-1-butyl [4-(7-octen-yloxy)-biphenyl-4′-bicarbonyloxy]benzoate (**11**), 4-(S)-2-methyl-1-butyl [4-(9-decen-1-yloxy)-biphenyl-4′-carbonyloxy]benzoate (**12**), 4-(S)-1-methyl-1-heptyl [4-(4-penten-1-yloxy)-biphenyl-4′-carbonyloxy]benzoate (**13**), 4-(S)-1-methyl-1-heptyl [4-(5-hexen-1-yloxy)-biphenyl-4′-carbonyloxy]benzoate (**14**), 4-(S)-1-methyl-1-heptyl [4-(7-octen-1-yloxy)-biphenyl-4′-carbonyloxy]benzoate (**15**), and 4-(S)-1-methyl-1-heptyl [4-(9-decen-1-yloxy)-biphenyl-4′-carbonyloxy]benzoate (**16**)*

These compounds were synthesized by similar methods. Using **12** as an example, in a two-necked glass reactor were placed compound **8** (2·470 g, 0·007 mol), compound **1** (2·084 g, 0·0098 mol), DCC (2·098 g, 0·0098 mol), several drops DMAP, and 70 ml dried methylene chloride. The mixture was allowed to react at room temperature and monitored with TLC until the reaction was complete. The products were first purified by column chromatography, and then recrystallized from *n*-hexane/ethyl acetate or methylene chloride to obtain needle-like solids. The yields, optical rotations ($[\alpha]_D^{25}$), and ^{1}H NMR data are listed in table 3.

Downloaded At: 19:46 25 January 2011

References

[1] Meyer, R. B., Liebert, L., Strzelecki, L., and Keller, P., 1975, *J. Phys. Lett.*, **36,** 69.

[2] Clark, N. A., and Lagerwall, S. T., 1980, *Appl. Phys. Lett.*, **36,** 898.

[3] Leslie, T. M., 1984, *Ferroelectrics*, **58,** 9.

[4] Furakawa, K., Terashima, K., Ichihashi, M., Inoue, H., Saito, S., and Inukai, T., 1985, 6th Liq. Cryst. Conf. Soc. Count., Halle (GDR), Abstract. A37.

[5] Furukawa, K., and Terashima, K., 1986, European Patent Application EP178647.

[6] Keller, P., 1984, *Mol. Cryst. liq. Cryst.*, **102,** 295.

[7] Koden, M., Ktsuse, H., Itoh, N., Kaneko, T., Tamai, K., Takeda, H., Shiomi, M., Numao, N., Kido, M., Matsuki, M., Miyoshi, S., and Wada, T., 1993, Fourth International Conference on Ferroelectric Liquid Crystals, Abstract p-147, p. 369.

[8] Tajima, E., Kondoh, S., and Suzuki, Y., 1993, Fourth International Conference on Ferroelectric Liquid Crystals, Abstract p-147, p. 371.

[9] Adams, T. G., and Sinta, R., 1989, *Mol. Cryst. liq. Cryst.*, **177,** 145.

[10] Scherowsky, G., Schliwa, A., Springer, J., Kuhnpast, K., and Trapp, W., 1989, *Liq. Cryst.*, **5,** 1281.

[11] Shibaev, V. P., Kozlovsky, M. V., and Plate, N. A., 1990, *Liq. Cryst.*, **8,** 1281.

[12] Vallerien, S. U., Kremer, F., and Fischer, E. W., 1990, *Makromol. Chem. rapid Commun.*, **11,** 593.

[13] Kapizta, H., and Zentel, R., 1991, *Makromol. Chem.*, **192,** 1859.

[14] Chen, J.-H., Chang, R.-C., Hsiue, G.-H., and Wu, S.-L., 1995, *Liq. Cryst.*, **18,** 291.

[15] Chen, J.-H., Hsiue, G.-H., Hwang, C.-P., and Wu, J.-L., 1995, *Liq. Cryst.*, **19,** 803.

[16] Hsiue, G.-H., Hwang, C.-P., Chen, J.-H., and Chang, R.-C., 1996, *Liq. Cryst.*, **20,** 45.

[17] Hsiue, G.-H., Wu, J.-L., and Chen, J.-H., 1996, *Liq. Cryst.*, **21,** 449.

[18] Kapitza, H., Zentel, R., Twieg, R. J., Nguyen, H. T., Vallerien, S., and Kremer, F., 1990, *Adv. Mater.*, **2,** 539.